Journal of Translational Medicine

RESEARCH

Open Access

Cancer-associated fibroblasts promote doxorubicin resistance in triple-negative breast cancer through enhancing ZFP64 histone lactylation to regulate ferroptosis

KeJing Zhang[1,2], Lei Guo[1,2], Xin Li[1,2], Yu Hu[1,2] and Na Luo[1,2,3*]

Abstract

Background Cancer-associated fibroblasts (CAFs) have been identified to drive chemotherapy resistance in triple-negative breast cancer (TNBC). This study evaluated the functions of CAFs-mediated suppressive ferroptosis in doxorubicin (DOX) resistance in TNBC and its detailed molecular mechanisms.

Methods TNBC cell lines were co-cultured with CAFs isolated from DOX-sensitive (CAF/S) or DOX-resistant (CAF/R) breast cancer tissues. Cell viability and death were assessed by cell counting Kit-8 (CCK-8) and propidium iodide (PI) staining. Ferroptosis was evaluated by detection of Fe^{2+}, malondialdehyde (MDA), glutathione (GSH), and lipid reactive oxygen species (ROS) levels. Histone lactylation was determined by lactate production, pan-Kla and H3K18la expression. Molecular mechanism was determined by chromatin immunoprecipitation (ChIP) and dual luciferase reporter system. Molecule and protein expression was detected by quantitative Real-Time PCR (RT-qPCR), Western blotting, immunofluorescence and immunohistochemical staining. TNBC cells were injected into the mammary fat pad of nude mice to investigate DOX sensitivity in vivo.

Results CAFs-derived lactate repressed ferroptosis to confer resistance of TNBC cells to DOX. Moreover, zinc finger protein 64 (ZFP64) expression was elevated in DOX-resistant TNBC and was associated with high histone lactylation level. CAFs facilitated histone lactylation to enhance ZFP64 expression, which triggered ferroptosis inhibition and DOX resistance. In addition, ZFP64 bound to the promoters of GTP cyclohydrolase-1 (GCH1) and ferritin heavy chain 1 (FTH1), thereby promoting their expression. Rescue experiments indicated that ZFP64 silencing-induced ferroptosis and high sensitivity of TNBC cells to DOX could be counteracted by GCH1 or FTH1 overexpression.

Conclusion CAFs acted as a ferroptosis inhibitor to cause DOX resistance of TNBC via histone lactylation-mediated ZFP64 up-regulation and subsequent promotion of GCH1-induced lipid peroxidation inhibition and FTH1-induced intracellular Fe^{2+} consumption.

Keywords CAFs, DOX resistance, TNBC, Ferroptosis, Histone lactylation, ZFP64

*Correspondence:
Na Luo
luonaxy2012@163.com
[1]Department of General Surgery, Xiangya Hospital, Central South University, Changsha, Hunan Province 410008, P.R. China
[2]Clinical Research Center For Breast Cancer Control and Prevention In Hunan Province, Changsha, Hunan Province 410008, P.R. China
[3]Department of General Surgery, Xiangya Hospital, Central South University & Clinical Research Center For Breast Cancer Control and Prevention In Hunan Province, No. 87, Xiangya Road, Changsha, Hunan Province 410008, P.R. China

© The Author(s) 2025. **Open Access** This article is licensed under a Creative Commons Attribution-NonCommercial-NoDerivatives 4.0 International License, which permits any non-commercial use, sharing, distribution and reproduction in any medium or format, as long as you give appropriate credit to the original author(s) and the source, provide a link to the Creative Commons licence, and indicate if you modified the licensed material. You do not have permission under this licence to share adapted material derived from this article or parts of it. The images or other third party material in this article are included in the article's Creative Commons licence, unless indicated otherwise in a credit line to the material. If material is not included in the article's Creative Commons licence and your intended use is not permitted by statutory regulation or exceeds the permitted use, you will need to obtain permission directly from the copyright holder. To view a copy of this licence, visit http://creativecommons.org/licenses/by-nc-nd/4.0/.

Introduction

Breast cancer remains the most frequent malignancy of women in the world. Triple-negative breast cancer (TNBC) is an aggressive type of breast cancer, featured by negative expression of estrogen receptor, progesterone receptor and epidermal growth factor receptor-2 [1]. Approximately 20% of breast cancer patients are diagnosed with TNBC, which are most likely to suffer drug resistance and metastasis, leading to a poor prognosis [2, 3]. Doxorubicin (DOX) has been widely used in TNBC chemotherapy because of its good efficacy [4]. However, DOX resistance greatly reduces its efficacy and limits its clinical application [5]. Therefore, understanding the mechanisms through which TNBC cells acquire DOX resistance is crucial to develop strategies to improve chemosensitivity.

Ferroptosis is a newly discovered type of iron-dependent cell death caused by ferrous ion accumulation, which is featured by lipid reactive oxygen species (ROS) overproduction [6]. Ferroptosis has close association with the malignant development of diverse malignancies, including TNBC [7, 8]. Notably, ferroptosis inhibition could confer DOX resistance in TNBC [9, 10]. Cancer-associated fibroblasts (CAFs), widely existed in tumor microenvironment, contribute to drug resistance and aggressiveness of cancer cells [11]. It is well established that CAFs can support TNBC growth through protect TNBC cells from DOX chemotherapy. For instance, Amornsupak et al. documented that CAFs induced high-mobility group box-1 (HMGB1) expression and consequently promoted DOX resistance in TNBC cells [12]. Inhibition of generation of CAFs by gamma mangostin could improve DOX sensitivity of TNBC cells [13]. CAFs can affect the efficacy of chemotherapy via various mechanisms. For example, CAFs can secrete multiple growth factors, cytokines, chemokines, pro-tumorigenic molecules, and extracellular vesicles that modulate the sensitivity of cancer cells to chemotherapy [14, 15]. In addition, CAFs could repress ferroptosis to trigger resistance of pancreatic cancer cells to gemcitabine [16]. So far, the influence of CAFs on ferroptosis during DOX resistance of TNBC cells has not been clarified. Therefore, a more thorough understanding of the mechanisms by which CAFs drive TNBC cell resistance is necessary to combat DOX resistance and malignant development in TNBC.

Histone lactylation, dose-dependently related to lactate level, is a key epigenetic modification that contributes to target gene transcription. Several studies have suggested the tumor-promotive role of histone lactylation [17, 18]. A previous study showed that high histone lactylation level indicated a poor prognosis, and histone lactylation facilitated tumorigenesis of ocular melanoma by up-regulating YTH m6A RNA-binding protein 2 (YTHDF2) [19]. Of note, Sun et al. found that hypoxic CAFs promoted lactate production, which drove breast cancer cell metastasis [20]. However, whether CAFs can affect lactylation and its involvement in ferroptosis during DOX resistance of TNBC cells are largely unknown.

Zinc finger protein 64 (ZFP64) belongs to the zinc-finger type C2H2 transcription factor family. As a transcription factor, ZFP64 could promote the progression of various malignancies, such as gallbladder cancer [21], esophageal cancer [22], and hepatocellular carcinoma [23]. Notably, a previous study reported that ZFP64 caused nab-paclitaxel resistance in gastric cancer progression [24]. As analyzed by GEPIA, UALCAN and Kaplan-Meier Plotter databases, ZFP64 was highly expressed in breast cancer, which was correlated with advanced tumor stage, a higher lymph node metastasis stage, and a poor prognosis of patients. In addition, JASPAR and hTFtarget databases predicted that ZFP64 might bind to the promoters of ferroptosis-related genes, including glutathione peroxidase 4 (GPX4), solute carrier family 7 member 11 (SLC7A11), ferritin heavy polypeptide 1 (FTH1), nuclear receptor coactivator 4 (NCOA4), acyl-CoA synthetase long-chain family member 4 (ACSL4), arachidonic acid 15-lipoxygenase (ALOX15), and GTP cyclohydrolase-1 (GCH1). Thus, we focused on ZFP64 and further elucidated its influence on TNBC progression. So far, whether ZFP64 can be modulated by lactylation to affect DOX resistance in TNBC has not been explored.

In this study, we sought to verify the role of CAFs-modulated ZFP64 in DOX resistance of TNBC cells. We found that CAFs-mediated lactylation up-regulated ZFP64 to inhibit ferroptosis via promoting GCH1-mediated lipid peroxidation inhibition and FTH1-mediated Fe^{2+} depletion, which conferred DOX resistance of TNBC cells. Our findings explained the novel mechanisms through which CAFs favored DOX resistance in TNBC, and identified promising target to increase chemosensitivity of TNBC patients.

Materials and methods

Clinical samples

60 patients with breast carcinoma (containing 30 DOX-sensitive and 30 DOX-resistant samples) at Xiangya Hospital, Central South University provided breast cancer tissues. Before surgical resection, the patients received DOX-based chemotherapy. As previously described [25], 30 patients were defined as DOX-resistant group, who suffered early recurrence within 6 months after DOX chemotherapy, and 30 patients were considered as DOX-sensitive group, who did not suffer tumor recurrence during follow-up period. The clinicopathological parameters of the breast cancer patients are shown in Table S1. Written informed consent was collected from

all participants. This study was approved by the Xiangya Hospital, Central South University.

Data retrieval and analysis

ZFP64 expression in diverse types of human cancers was analyzed by GEPIA database (http://gepia2.cancer-pku.cn/#index). UALCAN database (https://ualcan.path.uab.edu/index.html) evaluated ZFP64 expression in normal and breast cancer patients in stages 1, 2, 3, 4 and different lymph node metastasis stages (N0, N1, N2, N3). The correlation between ZFP64 expression and overall survival (OS), recurrence-free survival (RFS), and distant metastasis-free survival (DMFS) of breast cancer patients was analyzed by Kaplan-Meier Plotter database (https://kmplot.com/analysis/index.php?p=background).

Isolation of CAFs

We extracted CAFs from DOX-sensitive and DOX-resistant breast cancer tissues. Briefly, the breast cancer tissues were cut up into pieces, followed by digestion with collagenase (100 μg/mL) and hyaluronidase (100 μg/mL) for 2 h at 37 °C. The collected CAFs after centrifugation were maintained in DMEM (Thermo Fisher, Waltham, MA, USA) containing 20% fetal bovine serum (FBS) (Thermo Fisher) at 37 °C with 5% CO_2. After washing with culture medium, the adherent CAFs were further identified by specific markers as described below.

Immunofluorescence staining

The primary CAFs were seeded onto coverslips, fixed with 4% paraformaldehyde, permeabilized with 0.2% Triton X-100, and blocked with 10% goat serum for 60 min. Incubation with smooth muscle actin-alpha (α-SMA) (A17910, 1:50, ABclonal, Wuhan, China), fibroblast activated protein (FAP) (A23789, 1:50, ABclonal), and FSP1 (A19109, 1:50, ABclonal) was performed at 4 °C overnight. Breast cancer tissues were fixed in 4% paraformaldehyde, dehydrated, and embedded in paraffin, sectioned into 5 μm-sections, and received antigen retrieval. The tissue samples were incubated with pan-Kla (PTM-1401RM, 1:50, PTM BioLab, Hangzhou, China), ZFP64 (55734-MSM1-P0, 1:10, Thermo Fisher), and H3K18la (PTM-1406RM, 1:500, PTM BioLab, Hangzhou, China) at 4 °C overnight. Then, the CAFs and tissue samples were probed with the specific secondary antibodies for 1 h, and examined under a fluorescent microscope (Olympus, Tokyo, Japan).

Cell culture and treatment

American Type Culture Collection (ATCC) (Manassas, VA, USA) provided BT-549 and MDA-MB-231 cells that were cultured in RPMI-1640 and DMEM containing 10% FBS, respectively. All cells grew at 37 °C with 5% CO_2. We added 0.5 μM DOX hydrochloride (MCE, Shanghai, China), 20 mM oxamate (Sigma-Aldrich, Saint Louis, MO, USA), 25 mM lactic acid (LA, Sigma-Aldrich), 5 μm Ferrostain-1 (Fer-1, MCE), 0.1 mM deferoxamine (DFO, MCE), 10 μM Z-VAD-FMK (MCE), 10 μM Necrostain-1 (Nec-1, MCE) to BT-549 and MDA-MB-231 cells, respectively.

Co-culture assay

We planted TNBC cells (5×10^4) into the lower chambers and CAFs (5×10^4) into the upper chambers of 0.4 mm Transwell chambers (Thermo Fisher) to establish a co-culture system. After co-culture for 48 h, TNBC cells were obtained for further examination.

Cell transfection

Genechem (Shanghai, China) provided short hairpin RNA (shRNA) targeting ZFP64 (shZFP64 sequence: GCAAGCAGCAGTTTAACAACC) and negative control shRNA (shNC sequence: GTTCTCCGAACGTGTCACGT). We inserted the full-length sequences of GCH1 or FTH1 into pcDNA3.1 to construct pcDNA3.1-GCH1 or FTH1 overexpression plasmid. TNBC cells (4×10^5) were transfected with shRNA or constructed plasmid using Lipofectamine 2000 (Thermo Fisher) for 48 h. We co-transfected lentivirus vector GV115-shZFP64 (Genechem), pHelper 1.0 and pHelper 2.0 plasmids into HEK-293T cells to produce lentivirus particles carrying shZFP64, named as lv-shZFP64. Lv-shNC served as the control lentiviruses. We infected lv-shZFP64 or lv-shNC into TNBC cells in the presence of polybrene, and selected the stably infected cells by puromycin (2 μg/mL) for 4 weeks.

Detection of lactate production

The Lactate Assay Kit (Abcam, Cambridge, UK) determined lactate content in the cellular supernatants. We detected the absorbance at 450 nm according to the manufacturer's protocol.

Cell counting Kit-8 (CCK-8)

The CCK-8 Kit (Abcam) examined the cell viability. In brief, TNBC cells were planted into 96-well plates (3×10^4 cells per well). Subsequently, we added 10 μL/well reaction solution into the wells, followed by incubation for 2 h at 37 °C. A microplate reader (Thermo Fisher) measured the absorbance at 460 nm. **Propidium iodide (PI) staining** PI staining evaluated cell death. The collected TNBC cells were stained with PI solution for 15 min in the dark. After adding with binding Buffer, a flow cytometer (BD, Franklin lakes, NJ, USA) detected the fluorescence of 10,000 cells.

Detection of glutathione (GSH), malondialdehyde (MDA), ferrous iron (Fe^{2+})

The Reduced GSH Content Assay Kit (Solarbio, Beijing, China), MDA Content Assay Kit (Solarbio), Ferrous Ion Content Assay Kit (Solarbio) analyzed the levels of GSH, MDA, and Fe^{2+}, following the product instructions.

Measurement of lipid ROS

The C11-BODIPY 581/591 probe (Thermo Fisher) measured the lipid ROS generation. In short, TNBC cells suspended in serum-free medium were stained with 2 μM C11-BODIPY 581/591 probe at 37 °C for 30 min. Subsequently, a flow cytometer analyzed the fluorescence in TNBC cells.

Transmission electron microscope (TEM)

TEM observed the mitochondrial morphology of TNBC cells. TNBC cells were subjected to fixation with 2.5% glutaraldehyde, followed by treatment with 1% osmium acid, dehydration, and embedding molds. After staining with lead citrate and uranyl acetate, a TEM (HITACHI, Tokyo, Japan) observed the mitochondrial morphology.

Chromatin immunoprecipitation (ChIP)

The ChIP Assay Kit (Beyotime, Shanghai, China) validated the binding of ZFP64 to FTH1/GCH1 promoter, and H3K18la modification in ZFP64 promoter. After crosslinking with 1% formaldehyde, TNBC cell lysates were sonicated to obtain chromatin fragments. ZFP64 antibody (17187-1-AP, Proteintech, Wuhan, China), H3K18la (PTM-1406RM, PTM BioLab) or IgG (30000-0-AP, Proteintech) immuno-precipitated the DNA-protein complexes overnight at 4 °C. The immuno-complexes were eluted to obtain DNA fragments, followed by Proteinase K treatment. qPCR detected the enrichment of FTH1/GCH1 promoter.

Dual luciferase reporter assay

We inserted the sequences containing the binding sites of ZFP64 to FTH1/GCH1 promoter into the pGL3-basic vector to construct luciferase reporter vectors. TNBC cells were transfected with shZFP64 combined with WT or luciferase reporter vector using Lipofectamine 2000. The Dual-Lucy Assay Kit (Solarbio) analyzed the luciferase activity.

Animal model

Slac Jingda Laboratory Animal Co., Ltd (Hunan, China) provided the BALB/c nude mice (Female, 6 weeks old). We injected BT-549 and MDA-MB-231 cells (5×10^6) stably transfected with shZFP64 or shNC mixed with or without CAF/R (ratio: 1:1) into the mammary fat pat of mice (6 mice per group). The formula: (length × width^2)/2 calculated tumor volume. Once the tumor volume reached 80–100 mm^3, we intraperitoneally injected vehicle or DOX (5 mg/kg) into the mice every 3 days for 6 times [26]. We sacrificed all mice after the injection for 25 days, and collected and weighed the tumors. The Experimental Ethics Committee Xiangya Hospital, Central South University approved the animal experiments.

Immunohistochemical staining

The tumors were embedded in paraffin and sectioned (5 μm). After deparaffinization and rehydration, the sections received antigen retrieval in boiled sodium citrate buffer. Treatment with 3% H_2O_2 blocked the endogenous peroxidase. The sections were probed with Ki-67 (A20018, 1:100, ABclonal), FTH1 (10727-1-AP, 1:50, Proteintech), GCH1 (28501-1-AP, 1:200, Proteintech), FAP (ab314456, 1:1000, Abcam), FSP1 (A19109, 1:200, ABclonal), CD29 (A23497, 1:1000, ABclonal), PDGFRβ (A2180, 1:50, ABclonal), CD8 (A23305PM, 1:500, ABclonal), CD31 (A19014, 1:500, ABclonal), CD206 (ab64693, 1:500, Abcam) overnight at 4 °C, followed by incubation with Biotin-conjugated secondary antibody (SA00004-2, 1:100, Proteintech). After reaction with diaminobenzidine (DAB), a light microscope photographed the immunohistochemical images. For CAF marker staining, CAF enrichment was evaluated by a histological score (H-score), defined by staining intensity (ranging from 0 to 4) multiplied by the percentage of stained sections, as described in a previous study [27].

Quantitative real-time PCR (RT-qPCR)

The RNA Easy Fast Isolation Kit (TIANGEN, Beijing, China) isolated total RNA, and the FastKing cDNA synthesis kit (cat. no. KR116-02, TIANGEN) transcribed the total RNA into cDNA. Real-time PCR was conducted using the Talent qPCR PreMix (SYBR Green) (cat. no. FP209-02, TIANGEN). $2^{-\Delta\Delta Ct}$ method quantified the relative mRNA expression normalized to GAPDH. Table S2 lists the primer sequences.

Western blotting

We extracted protein samples using the RIPA solution (Beyotime) and detected protein concentration using the BCA Protein Assay Kit (Beyotime). Sodium dodecyl sulfate polyacrylamide gel electrophoresis separated the protein samples (30 μg), followed by blotting onto polyvinylidene difluoride membranes. After blocking in 5% skim milk for 1 h, we incubated the membranes with primary antibodies against Pan Kla (PTM-1401RM, 1:500, PTM BioLab), H3K18la (PTM-1406RM, 1:500, PTM BioLab), ZFP64 (17187-1-AP, 1:500, Proteintech), GCH1 (28501-1-AP, 1:1000, Proteintech), FTH1 (10727-1-AP, 1:2000, Proteintech), glyceraldehyde-phosphate dehydrogenase (GAPDH) (AC001, 1:10000, ABclonal), Histone H3 (A2348, 1:2000, ABclonal) at 4 °C overnight.

Subsequently, after incubation with the HRP Goat Anti-Rabbit IgG (AS014, 1:2000, ABclonal), the ECL Western Blotting Substrate (Solarbio) developed the protein bands.

Statistical analysis

The measurement data are shown as mean ± standard deviation (SD). We conducted Student's t test for two group comparison or one-way analysis of variance (ANOVA) followed by Tukey's post hoc test for multiple comparisons using GraphPad Prism 8.0 software. $P < 0.05$ indicated as statistically significant.

Results

CAFs-derived lactate repressed ferroptosis to reduce sensitivity of TNBC cells to DOX

First, we isolated CAFs from DOX-sensitive and DOX-resistant breast cancer tissues, and named as CAF/S and CAF/R, respectively. To categorize CAF populations, we detected the expression of CAFs markers, α-SMA, FAP, fibroblast specific protein-1 (FSP1), Integrin β1 (CD29), platelet derived growth factor receptor β (PDGFR β) in DOX-resistant TNBC samples. According to a decision tree algorithm for CAF subset enrichment [27], we found that DOX-resistant TNBC showed accumulation of CAF-S1 and CAF-S4 (Fig. S1A&B). The morphology of CAF/S and CAF/R was spindle-like, mixed with scalene triangular shape (Fig. S1C). The CAF/R exhibited higher expression of α-SMA, FAP, and FSP1 as compared with CAF/S (Fig. S1C). In addition, lactate level was higher in CAF/R than that in CAF/S (Fig. S1D). CCK8 data indicated that DOX sensitivity in TNBC cells was lowered by CAF/R co-culture or lactic acid (LA) treatment, but not significantly affected by CAF/S (Fig. S1E). Oxamate, an inhibitor of lactate production, could abolish CAF/R-induced DOX resistance (Fig. S1E). Furthermore, DOX-induced increase in cell death, MDA, Fe^{2+}, and lipid ROS levels was repressed by CAF/R or LA treatment, and Oxamate neutralized the effect of CAF/R (Fig. S1F-I). However, co-culture with CAF/S did not significantly influence these changes in DOX-treated TNBC cells (Fig. S1F-I). These data suggested that CAFs contributed to DOX and ferroptosis resistance in TNBC cells through delivering lactate.

ZFP64 was up-regulated in DOX-resistant TNBC tissues, which was correlated with elevated histone lactylation level

Since lactate is recognized as a crucial substrate of histone lactylation, we determined the histone lactylation level in DOX-sensitive and DOX-resistant clinical samples. Immunofluorescence staining of pan-Kla showed a higher global lactylation level in DOX-resistant tissues in comparison with DOX-sensitive tissues (Fig. 1A&B). Western blotting further demonstrated that pan-Kla and H3K18la protein levels were elevated in DOX-resistant group (Fig. 1C). As analyzed by GEPIA database, ZFP64 is overexpressed across most types of human cancers, including breast cancer (Fig. S2A). Consistently, UALCAN database indicated that ZFP64 was up-regulated in breast cancer (Fig. S2B). Moreover, high ZFP64 expression suggested an advanced tumor stage and a higher lymph node metastasis stage (Fig. S2C&D). In addition, Kaplan-Meier Plotter database showed that high expression of ZFP64 was correlated with lower overall survival (OS), recurrence-free survival (RFS), and distant metastasis-free survival (DMFS) of breast cancer patients (Fig. S2E-G). Therefore, ZFP64 was focused on in the following experiments. Intriguingly, ZFP64 mRNA level was increased in DOX-resistant patients as compared with DOX-sensitive patients (Fig. 1D). In addition, up-regulation of ZFP64 was positively correlated with lactylation level in DOX-resistant tissues (Fig. 1E). Consistently, we observed a higher protein level of ZFP64 in DOX-resistant group (Fig. 1F). More importantly, immunofluorescence staining validated the co-localization of ZFP64 and H3K18la in DOX-sensitive samples, which was strengthened in DOX-resistant samples (Fig. 1G). These findings indicated that up-regulation of ZFP64 had close association with histone lactylation in DOX-resistant TNBC samples.

CAFs-derived lactate enhanced ZFP64 expression via promoting its histone lactylation

We further explored whether CAFs modulated ZFP64 expression through histone lactylation. Notably, the mRNA and protein levels of ZFP64 were remarkably raised in TNBC cells treated with LA or co-cultured with CAF/R, which was not significantly affected by CAF/S. Whereas oxamate-mediated inhibition in lactate production abrogated the promotive effect of CAF/R on ZFP64 expression (Fig. 2A&B). Accordingly, LA administration or co-culture with CAF/R strikingly up-regulated pan-Kla and H3K18la in TNBC cells, which was reversed by oxamate treatment (Fig. 2C). However, CAF/S did not evidently enhance pan-Kla and H3K18la expression in TNBC cells (Fig. 2C). ChIP assay showed that the binding of ZFP64 promoter to H3K18la protein was heightened by LA, CAF/R or CAF/S co-culture (Fig. 2D). CAF/S-mediated promotive effect was less obvious than that of CAF/R, and oxamate abolished CAF/R-mediated the above change (Fig. 2D). The above results indicated that CAF/R facilitated ZFP64 expression via up-regulating histone lactylation level in TNBC cells.

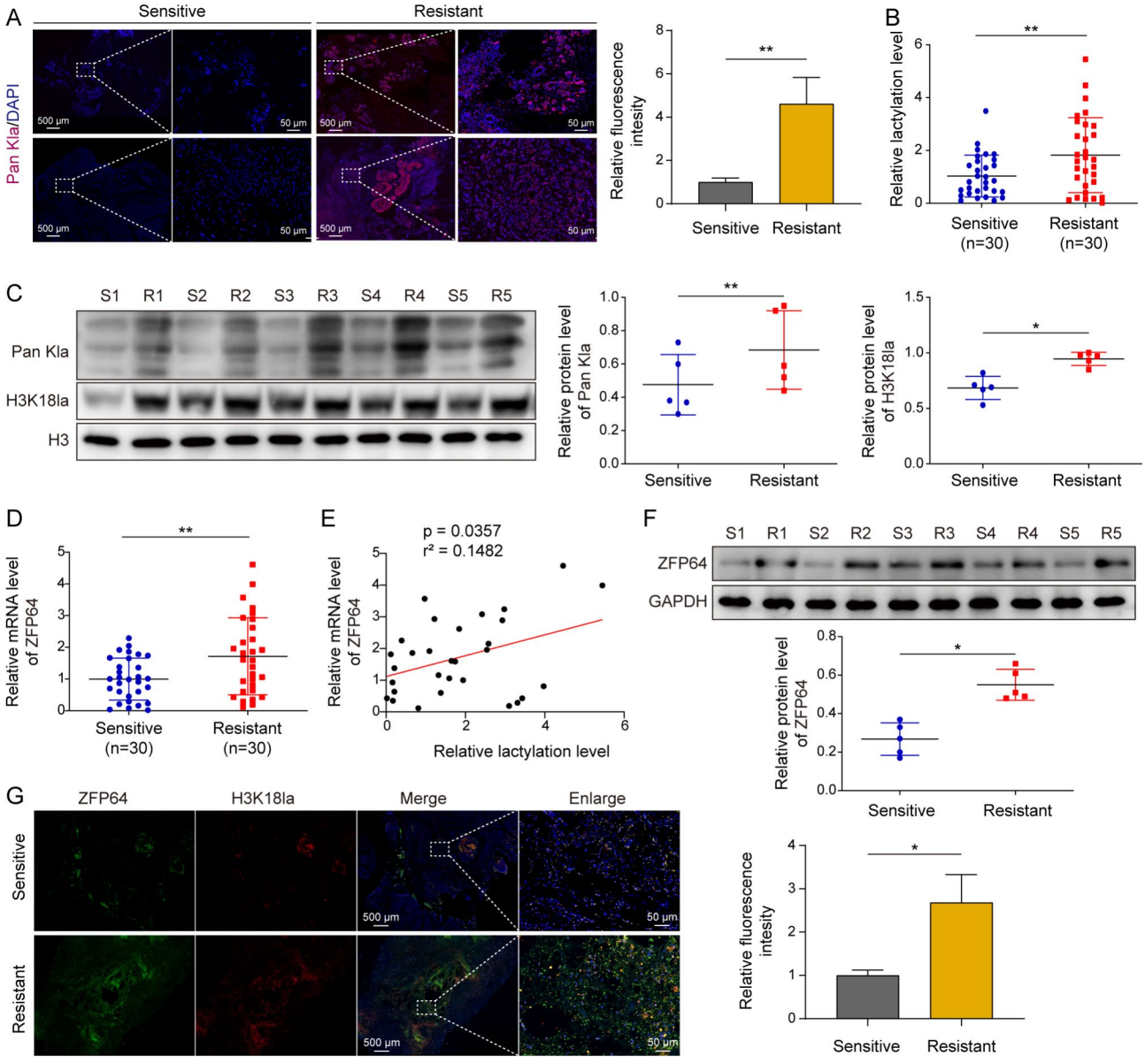

Fig. 1 Up-regulation of ZFP64 in DOX-resistant TNBC tissues was positively associated with high histone lactylation level. (**A**&**B**) Pan-Kla level in DOX-resistant/sensitive TNBC tissues was evaluated by immunofluorescence staining. (**C**) The protein levels of pan-Kla and H3K18la in DOX-resistant/sensitive TNBC tissues were assessed by Western blotting. (**D**) RT-qPCR analysis of ZFP64 mRNA expression in DOX-resistant/sensitive TNBC tissues. (**E**) Pearson correlation test analyzed the correlation between ZFP64 and lactylation levels. (**F**) Western blotting determined ZFP64 protein abundance in DOX-resistant/sensitive TNBC tissues. (**G**) Co-localization of ZFP64 and H3K18la in DOX-resistant/sensitive TNBC tissues was observed by immunofluorescence staining. Student's t test was performed for statistical analysis. *$p < 0.05$, **$p < 0.01$, ***$p < 0.001$

Knockdown of ZFP64 raised DOX sensitivity in TNBC cells through inducing ferroptosis

Given that ZFP64 expression was promoted by CAF/R via histone lactylation, the influence of ZFP64 on DOX sensitivity in TNBC cells was further investigated. shZFP64-mediated silencing of ZFP64 was validated in TNBC cells (Fig. S3A&B). The sensitivity of TNBC cells to DOX was enhanced after ZFP64 depletion, which was counteracted by ferroptosis inhibitor Fer-1 or DFO, but not affected by apoptosis inhibitor Z-VAD-FMK or necrosis inhibitor Nec-1 (Fig. S3C). This result implied that ZFP64 might regulate DOX sensitivity via modulation of ferroptosis, instead of apoptosis or necrosis. Besides, the increased cell death percentage, MDA, Fe^{2+}, and lipid ROS levels, and decreased GSH level in DOX-exposed TNBC cells were reinforced by ZFP64 down-regulation (Fig. S3D-H). Additionally, TME analysis showed that ZFP64 deficiency further heightened DOX-induced reduction in mitochondrial area and increase in mitochondrial density

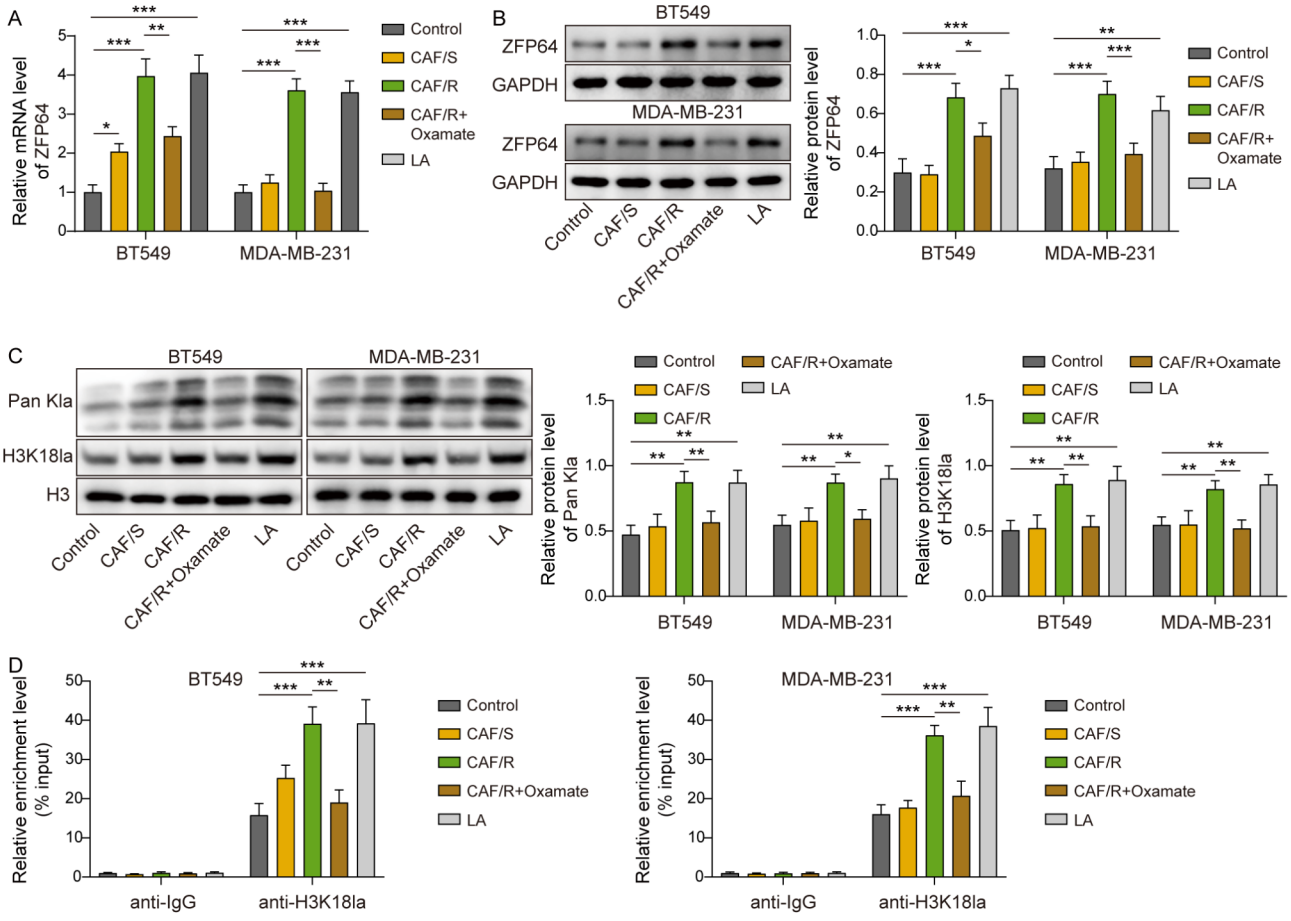

Fig. 2 ZFP64 expression was increased by CAFs-mediated histone lactylation. (**A**&**B**) ZFP64 expression was measured by RT-qPCR and Western blotting in TNBC cells co-cultured with or without CAF/S or CAF/R were treated with or without 20 mM oxamate or 25 mM LA for 48 h. (**C**) Western blotting analysis of Pan-Kla and H3K18la protein levels in TNBC cells co-cultured with or without CAF/S or CAF/R were treated with or without 20 mM oxamate or 25 mM LA for 48 h. (**D**) ChIP assay validated the interaction between H3K18la and ZFP64 promoter in TNBC cells co-cultured with or without CAF/S or CAF/R were treated with or without 20 mM oxamate or 25 mM LA for 48 h. $n = 3$. One-way ANOVA was performed for statistical analysis. $^{*}p < 0.05$, $^{**}p < 0.01$, $^{***}p < 0.001$

of TNBC cells (Fig. S3I). Collectively, ZFP64 knockdown sensitized TNBC cells to DOX via ferroptosis induction.

ZFP64 down-regulation reversed CAFs-mediated DOX resistance in TNBC cells

To verify the involvement of ZFP64 in CAF/R-induced DOX resistance, TNBC cells transfected with shNC or shZFP64 were co-cultured with CAF/R. CCK-8 data demonstrated that CAF/R-mediated enhancement in DOX-treated cell viability was eliminated by ZFP64 deficiency (Fig. 3A). Furthermore, ZFP64 knockdown abolished CAF/R-induced inhibitory effect on cell death, production of MDA, Fe^{2+}, and lipid ROS, and promotive effect on GSH level in TNBC cells upon DOX exposure (Fig. 3B-F). Moreover, CAF/R co-culture alleviated DOX-triggered mitochondrial morphological changes, including mitochondrial diminution, ridge disappearance, and ruptured membranes; however, ZFP64 depletion counteracted CAF/R-induced the above changes (Fig. 3G). Taken together, these observations suggested that CAFs conferred DOX resistance in TNBC cells via modulation of ZFP64 expression.

ZFP64 facilitated the transcription and expression of ferroptosis-related molecules GCH1 and FTH1

To uncover the mechanism of ZFP64 in ferroptosis, we detected the expression of a series of ferroptosis-related molecules after silencing of ZFP64. As analyzed by RT-qPCR, GCH1 and FTH1 were lowly expressed in ZFP64-silenced TNBC cells, among which GCH1 and FTH1 were most significantly down-regulated (Fig. 4A). Whereas, SLC7A11, NCOA4, ACSL4, and ALOX15 levels were not significantly altered after ZFP64 knockdown (Fig. 4A). Besides, we observed higher levels of GCH1 and FTH1 in DOX-resistant patients as compared with DOX-sensitive patients (Fig. 4B&D), and there was a positive correlation between GCH1/FTH1 and ZFP64 levels in DOX-resistant specimens (Fig. 4C&E). Further

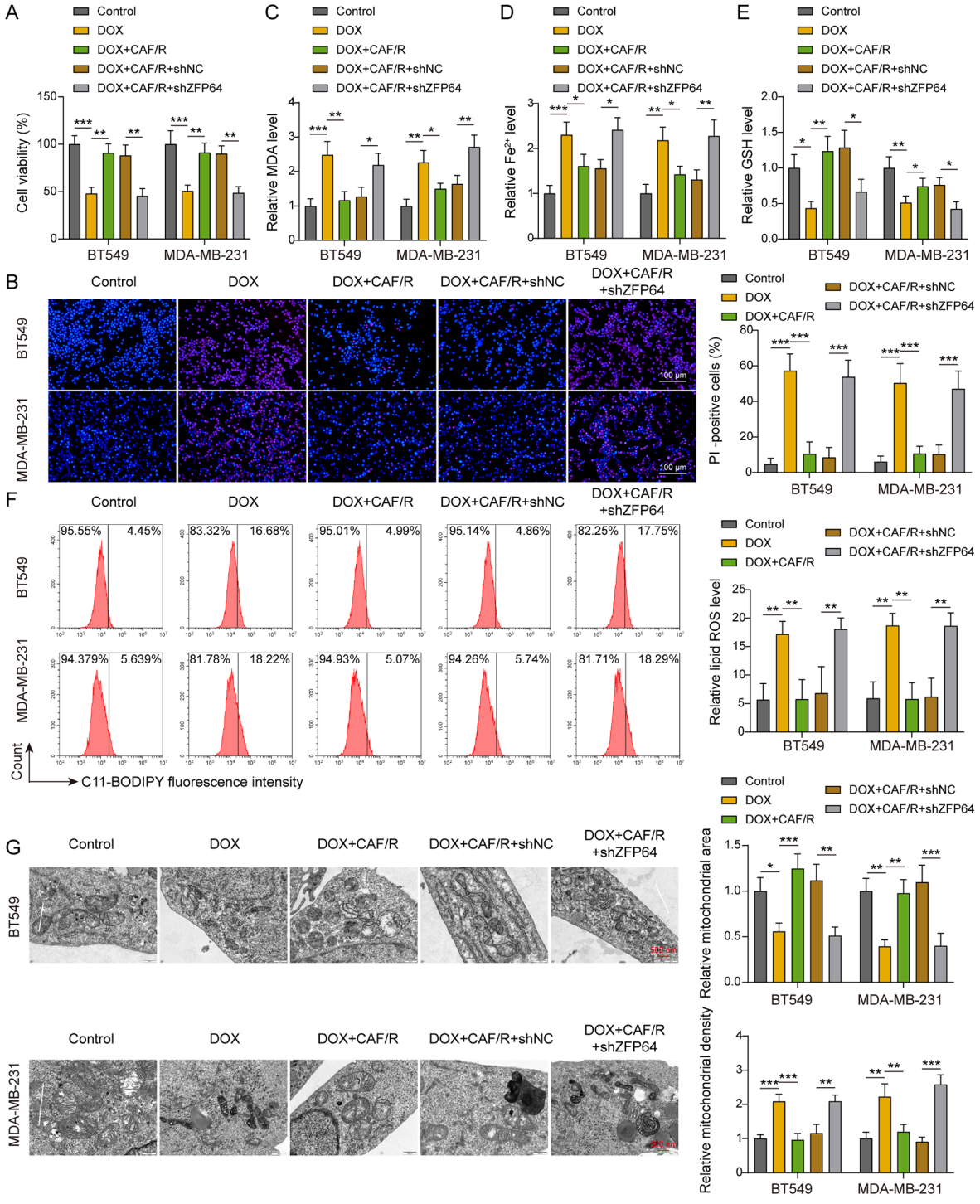

Fig. 3 ZFP64 knockdown counteracted CAFs-induced DOX insensitivity in TNBC cells. (**A**) CCK-8 determined the viability of DOX-treated TNBC cells co-cultured with or without CAF/R in combination with or without transfection with shNC or shZFP64. (**B**) Cell death was evaluated by PI staining via flow cytometry in DOX-treated TNBC cells co-cultured with or without CAF/R in combination with or without transfection with shNC or shZFP64. (**C**-**E**) MDA, Fe^{2+}, and GSH levels were detected in DOX-treated TNBC cells co-cultured with or without CAF/R in combination with or without transfection with shNC or shZFP64. (**F**) Lipid ROS production was detected by C11-BODIPY 581/591 probe via flow cytometry in DOX-treated TNBC cells co-cultured with or without CAF/R in combination with or without transfection with shNC or shZFP64. (**G**) Mitochondrial morphological changes were determined by TEM in DOX-treated TNBC cells co-cultured with or without CAF/R in combination with or without transfection with shNC or shZFP64. $n = 3$. One-way ANOVA was performed for statistical analysis. *$p < 0.05$, **$p < 0.01$, ***$p < 0.001$

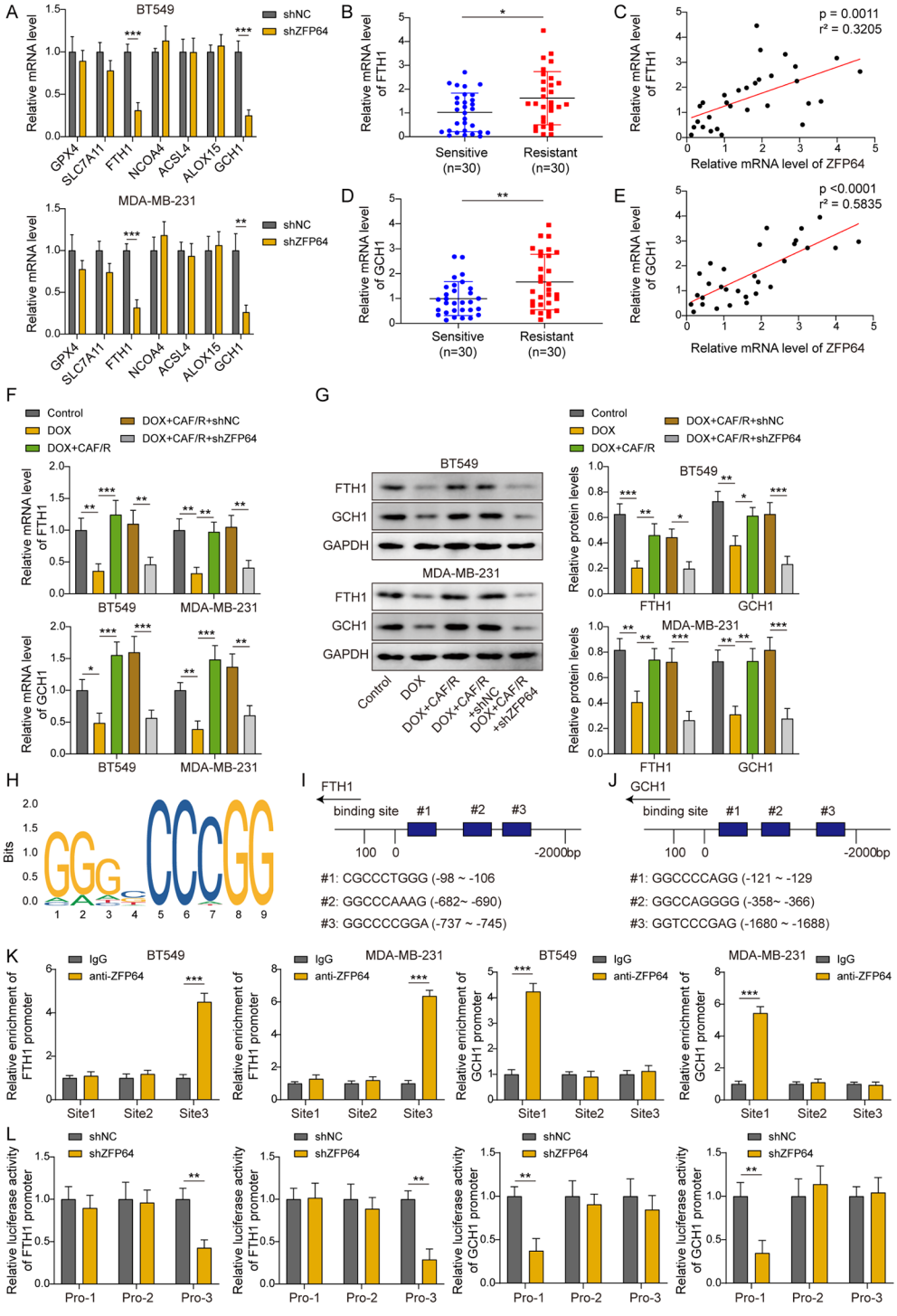

Fig. 4 ZFP64 directly bound to the promoters of GCH1 and FTH1 to promote their transcription. (**A**) Expression levels of ferroptosis-related molecules in TNBC cells were detected by RT-qPCR after transfection with shNC or shZFP64 for 48 h. (**B**) FTH1 level in DOX-resistant/sensitive TNBC tissues was evaluated by RT-qPCR. (**C**) Pearson correlation test detected the correlation between ZFP64 and FTH1 levels in DOX-resistant TNBC tissues. (**D**) RT-qPCR analysis of GCH1 level in DOX-resistant/sensitive TNBC tissues. (**E**) Pearson correlation test evaluated the correlation between ZFP64 and GCH1 levels in DOX-resistant TNBC tissues. (**F**&**G**) GCH1 and FTH1 expression was measured by RT-qPCR and Western blotting in DOX-treated TNBC cells co-cultured with or without CAF/R together with or without transfection with shNC or shZFP64. (**H**-**J**) JASPAR database predicted the potential binding sites of ZFP64 to GCH1 or FTH1 promoter. (**K**) The direct binding of ZFP64 to GCH1 or FTH1 promoter in TNBC cells was verified by ChIP. (**L**) The transcriptional activity of FTH1 or GCH1 in TNBC cells transfected with shNC or shZFP64 was determined by dual luciferase reporter assay. For A, F, G, K, L, $n = 3$. For B-E, $n = 30$. Student's t test (for B, D, K, L) and one-way ANOVA (for **A**, **F**, **G**) were performed for statistical analysis. *$p < 0.05$, **$p < 0.01$, ***$p < 0.001$

RT-qPCR and Western blotting results revealed that DOX-induced down-regulation of GCH1 and FTH1 in TNBC cells was recovered by CAF/R co-culture (Fig. 4F&G). Whereas ZFP64 deficiency abolished the promotive role of CAF/R in GCH1 and FTH1 expression (Fig. 4F&G). Notably, JASPAR database predicted that ZFP64 possessed three potential binding sites to GCH1 or FTH1 promoter (Fig. 4H-J). ChIP assay validated that ZFP64 could bind to FTH1 promoter (site 3) and GCH1 promoter (site 1) in TNBC cells (Fig. 4K). Consistently, the luciferase activities of FTH1 promoter (site 3) and GCH1 promoter (site 1) were strikingly reduced by ZFP64 silencing, whereas the luciferase activities of other binding sites to GCH1 or FTH1 promoter were not altered (Fig. 4L). Thus, ZFP64 directly bound to FTH1 promoter (site 3) and GCH1 promoter (site 1). To sum up, ZFP64 contributed to GCH1 and FTH1 transcription and expression, thereby causing ferroptosis inhibition in TNBC cells.

FTH1 or GCH1 overexpression counteracted the effect of ZFP64 silencing on ferroptosis and DOX sensitivity in TNBC cells

Since FTH1 or GCH1 could be directly modulated by ZFP64, we next investigated whether FTH1 or GCH1 was involved in the biological function of ZFP64 in DOX resistance. For this purpose, DOX-treated TNBC cells were transfected with shZFP64 together with or without FTH1 or GCH1 overexpression plasmid. The overexpression efficiency of FTH1 or GCH1 was verified in TNBC cells (Fig. 5A-D). After overexpressing FTH1 or GCH1 in TNBC cells, the promotive roles of shZFP64 in ferroptosis were compromised, including cell death (Fig. 5E&F), MDA (Fig. 5G), Fe^{2+} (Fig. 5H), GSH (Fig. 5I), and lipid ROS levels (Fig. 5J). In addition, ZFP64 knockdown-induced mitochondrial morphological changes in DOX-exposed TNBC cells were neutralized by co-transfection with FTH1 or GCH1 overexpression plasmid (Fig. 5K). Further Western blotting analysis showed that DOX-mediated down-regulation of GCH1 and FTH1 was intensified by ZFP64 depletion, which was abolished by enforced expression of FTH1 or GCH1 (Fig. 5L). Collectively, these findings proved that ZFP64 inhibition facilitated ferroptosis and DOX sensitivity through inhibiting FTH1-mediated Fe^{2+} depletion or GCH1-mediated inhibition of lipid peroxidation.

CAFs increased ZFP64 expression to inhibit ferroptosis, thereby causing DOX resistance in nude mice

To verify the regulatory role in DOX resistance in vivo, we established a xenograft model in nude mice. ZFP64 knockdown strengthened the anti-cancer effect of DOX treatment, as evidenced by slower growth rate, smaller tumor volume, and lighter tumor weight. However, CAF/R co-transplantation counteracted ZFP64 silencing-induced the above alterations (Fig. 6A-C). In addition, the increased MDA and Fe^{2+} levels and decreased GSH level in response to DOX therapy were promoted by ZFP64 deficiency, which could be abolished by CAF/R treatment (Fig. 6D-F). Subsequently, the expression of FTH1 and GCH1 was obviously decreased in tumors treated with DOX, which was further declined in ZFP64 silencing group (Fig. 6G-I). Whereas CAF/R co-transplantation reversed shZFP64-mediated FTH1 and GCH1 down-regulation (Fig. 6G-I). Moreover, immunohistochemical staining supported that ZFP64 depletion further enhanced DOX-induced decreased Ki-67, FTH1 and GCH1 expression in tumor tissues, which was abrogated in CAF/R co-treatment group (Fig. 6J). For tumor microenvironment characterization, the expression of CD8 (T cell marker), CD31 (vascularization marker) and CD206 (M2 macrophage marker) in tumors was detected by immunohistochemical staining. We found that the increased expression of CD8, and decreased expression of CD31 and CD206 in DOX treatment group were intensified by ZFP64 knockdown, and these changes were counteracted by CAF/R co-treatment (Fig. 6K). Therefore, our data indicated that ZFP64 up-regulated by CAF/R restrained ferroptosis to result in DOX resistance through activation of FTH1 and GCH1 in TNBC.

Discussion

Chemotherapy remains the main adjuvant therapy for TNBC patients [28]. However, a significant proportion of TNBC cells may develop drug resistance to cytotoxic chemotherapy [29], which greatly limit the effectiveness of chemotherapy and even result in treatment failure. Studies have suggested that ferroptosis inhibition is responsible for chemotherapy resistance [30, 31]. Ferroptosis promotion effectively enhanced the anti-cancer efficiency of DOX in TNBC cells [32]. Therefore, uncovering the molecular mechanisms of ferroptosis is undoubtedly a key way to overcome drug-resistance of TNBC. This study revealed for the first time that CAFs contributed to DOX resistance in TNBC cells by inducing ferroptosis. Mechanistically, CAFs released lactate to up-regulate ZFP64 via histone lactylation, and consequently led to GCH1 and FTH1 transcription and expression. Our findings elucidated novel regulatory mechanism for ferroptosis during DOX resistance, thereby suggesting ZFP64/GCH1 or FTH1 axis a key therapeutic target for conquering DOX resistance of TNBC.

CAFs within the tumor microenvironment have been recognized as a crucial contributor to chemoresistance. CAFs can secret multiple types of molecules and proteins that mediate the crosstalk with tumor cells [33]. A previous study showed that lactate derived from hypoxic CAFs exerted an intermediary role to contribute to

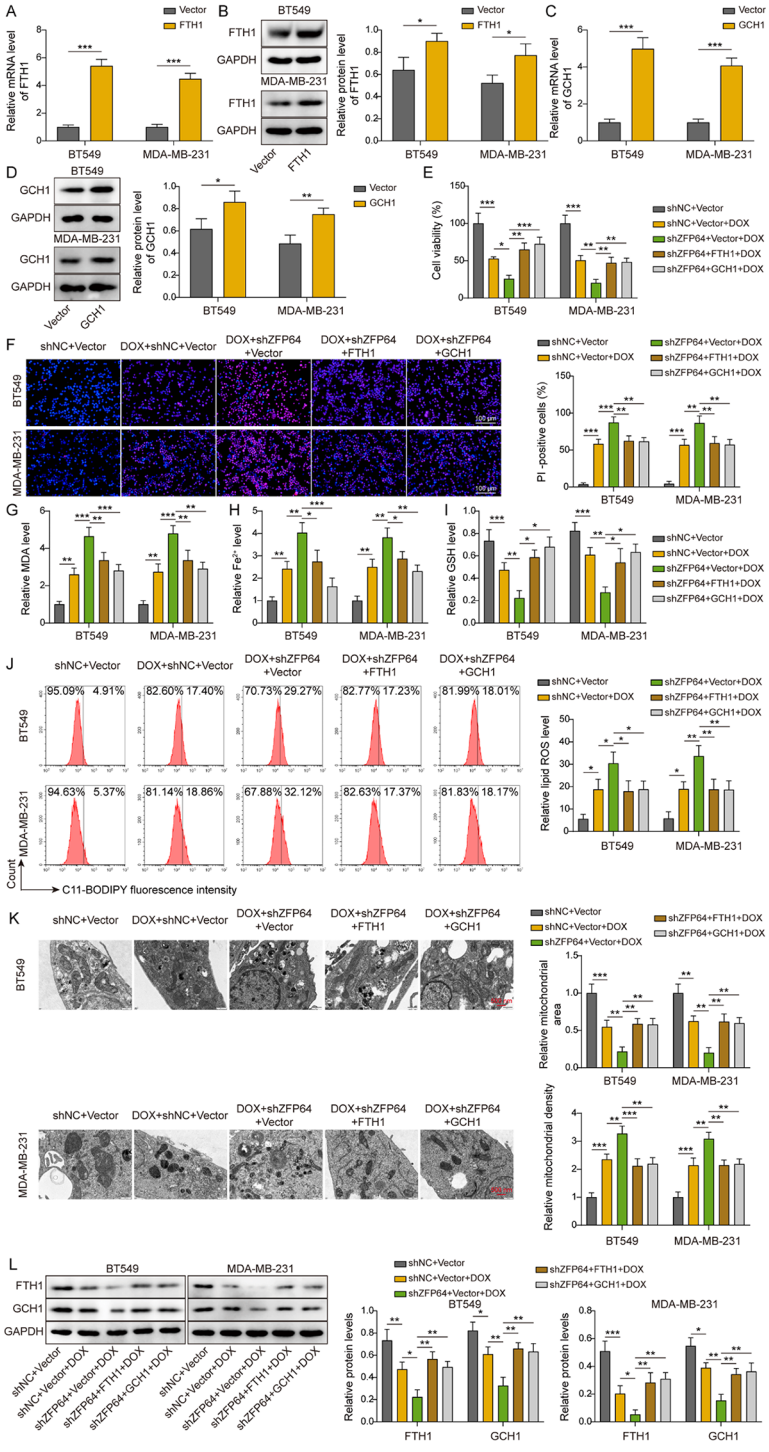

Fig. 5 FTH1 or GCH1 overexpression abolished shZFP64-mediated promotion in ferroptosis and DOX sensitivity in TNBC cells. (**A**-**D**) TNBC cells were transfected with vector, FTH1 or GCH1 overexpressing plasmid for 48 h. FTH1 and GCH1 expression in TNBC cells was assessed by RT-qPCR and Western blotting. (**E**) CCK-8 assay detected the viability of TNBC cells transfected with shZFP64 together with FTH1 or GCH1 overexpressing plasmid in the presence of DOX. (**F**) Cell death was determined by PI staining via flow cytometry in TNBC cells transfected with shNC or shZFP64 together with FTH1 or GCH1 overexpressing plasmid in the presence of DOX. (**G**-**I**) MDA, Fe^{2+}, and GSH levels were measured in TNBC cells transfected with shNC or shZFP64 together with FTH1 or GCH1 overexpressing plasmid in the presence of DOX. (**J**) Lipid ROS production was assessed by C11-BODIPY 581/591 probe via flow cytometry in TNBC cells transfected with shNC or shZFP64 together with FTH1 or GCH1 overexpressing plasmid in the presence of DOX. (**K**) Mitochondrial morphological changes were observed by TEM in TNBC cells transfected with shNC or shZFP64 together with FTH1 or GCH1 overexpressing plasmid in the presence of DOX. (**L**) The protein levels of FTH1 and GCH1 were detected by Western blotting in TNBC cells transfected with shNC or shZFP64 together with FTH1 or GCH1 overexpressing plasmid in the presence of DOX. $n = 3$. Student's t test (for A-D) and one-way ANOVA (for E-K) were performed for statistical analysis. $^{*}p < 0.05$, $^{**}p < 0.01$, $^{***}p < 0.001$

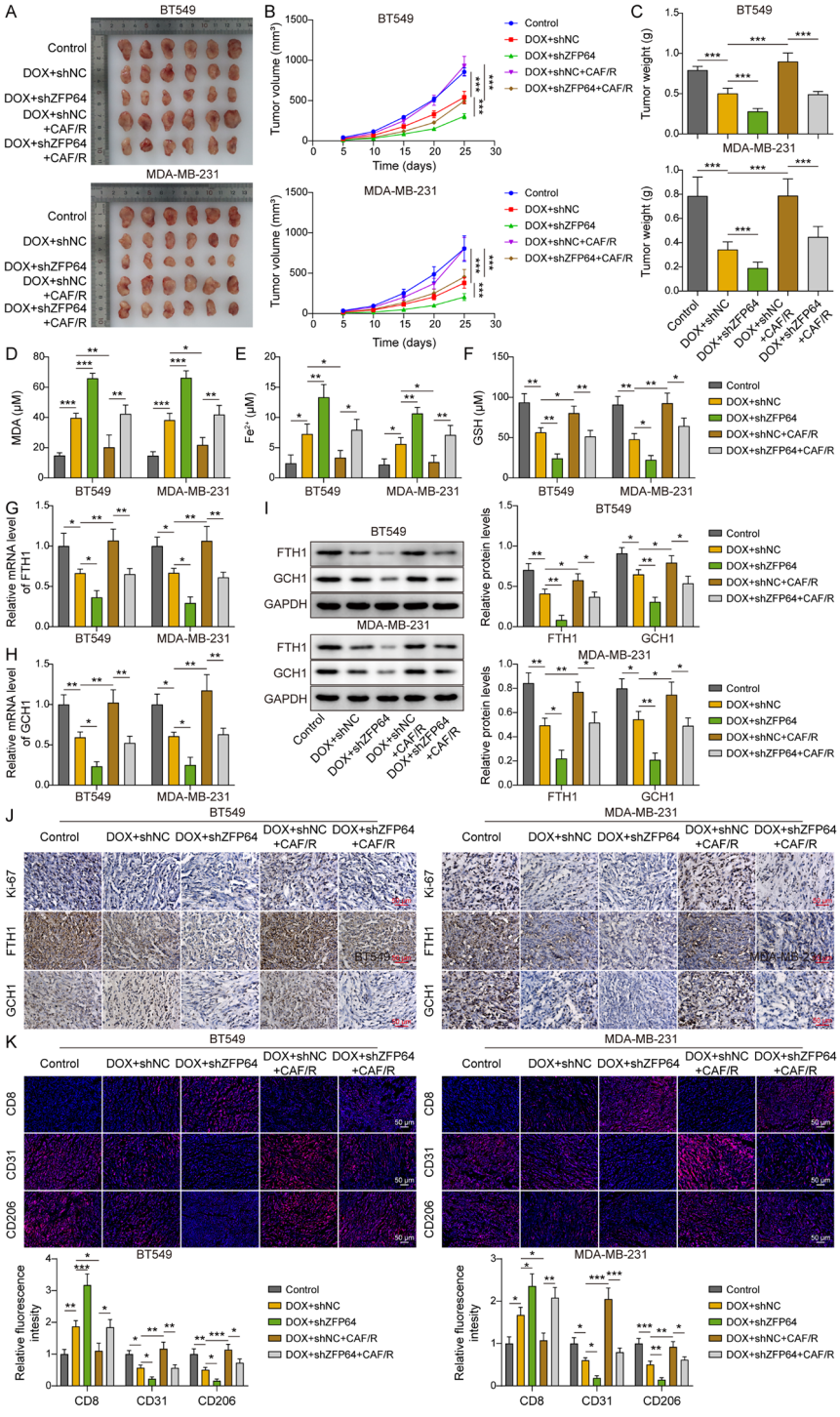

Fig. 6 CAFs up-regulated ZFP64 to repress ferroptosis, thereby leading to DOX resistance in vivo. BT-549 and MDA-MB-231 cells (5×10^6) were stably transfected with shZFP64 or shNC and mixed with or without CAF/R (ratio: 1:1) were injected into the mammary fat pat of mice, followed by intraperitoneal injected with vehicle or 5 mg/kg DOX. (**A**) The images of xenograft tumors in each group. (**B**&**C**) Tumor volume and weight were detected. (**D**-**F**) MDA, Fe^{2+}, and GSH levels in tumors were measured. (**G**-**I**) FTH1 and GCH1 expression in tumor tissues was assessed by RT-qPCR and Western blotting. (**J**) Immunohistochemical staining analyzed Ki67, FTH1 and GCH1 expression in tumors. (**K**) Immunohistochemical staining detected the expression of CD8 (T cell marker), CD31 (vascularization marker) and CD206 (M2 macrophage marker) in tumors. $n=6$. One-way ANOVA was performed for statistical analysis. $^*p<0.05$, $^{**}p<0.01$, $^{***}p<0.001$

metastasis of breast cancer cells [20]. Moreover, lactate-mediated interplay between CAFs and gastric cancer cells facilitated the development of anlotinib resistance [34]. Recently, the influence of CAFs on ferroptosis of cancer cells has been documented. For example, CAFs released exosomal miR-3173-5p to repress ferroptosis, thus inducing gemcitabine resistance in pancreatic ductal adenocarcinoma [16]. Another study found that miR-522 derived from CAFs led to ferroptosis resistance, and ultimately reduced chemo-sensitivity of gastric cancer cells [35]. So far, whether CAFs affect ferroptosis during the development of DOX resistance in TNBC cells has not been clarified. Although CAFs are the most prominent stromal components, characterizing their heterogeneity in cancers is necessary. A study analyzed CAF heterogeneity in TNBC via detection of CAFs markers αSMA, FAP, PDGFRβ, and FSP1 [27]. Consistent with the previous study, we found that CAF-S1 and CAF-S4 were enriched in DOX-resistant TNBC. Here, we provided first evidence that CAFs could restrain ferroptosis and drive DOX resistance in TNBC cells through lactate production.

Lactate-derived histone lactylation is a novel type of epigenetic regulation that directly facilitates gene transcription and expression [36]. Aerobic glycolysis-mediated increased histone lactylation has been reported to support c-Myc expression during breast cancer progression [37]. Notably, high lactate level promoted histone lactylation, which rendered chemotherapy insensitivity of colorectal tumor cells [38]. However, the involvement of lactate-mediated lactylation in chemotherapy insensitivity of TNBC cells remains largely unknown. Here, we first revealed that DOX resistant breast cancer tissues exhibited elevated histone lactylation level. Whether histone lactylation affected DOX resistance via modulation of target gene expression requires further explorations.

ZFP64 belongs to Krüppel C2H2-type zinc finger family. To date, the tumor-promoting roles of ZFP64 have been identified. As evaluated by genomic and proteomic analyses, ZFP64 was highly expressed in tumors in comparison with normal tissues [39, 40]. Wei et al. documented that ZFP64 was involved in the immune evasion and anti-PD1 resistance in tumorigenesis of hepatocellular carcinoma [23]. Of note, high ZFP64 expression accelerated gastric cancer development via promoting chemoresistance and cancer immunosuppression [24]. However, little is known about the role of ZFP64 in TNBC. In our study, up-regulation of ZFP64 was positively correlated with histone lactylation level in DOX resistant breast cancer. CAFs facilitated ZFP64 expression via histone lactylation, which suppressed ferroptosis to drive DOX insensitivity of TNBC cells. To incorporate TME characterization, we investigated the influence of ZFP64 on the expression of CD8 (T cell marker), CD31 (vascularization marker) and CD206 (M2 macrophage marker) in tumors. Our results proved that T cell and macrophage infiltration and vascularization were affected by ZFP64 during ferroptosis induction with DOX treatment.

Ferroptosis is a biological process modulated by various molecules. FTH1 is an inhibitor of ferroptosis through regulation of iron metabolism [41]. Degradation of FTH1 was reported to cause accumulation of intracellular Fe^{2+} and ultimately induce ferroptosis [42]. GCH1 is a new oncogene that suppresses lipid peroxidation to counteract ferroptosis [43]. GCH1 knockdown was reported to delay colorectal cancer growth via inducing ferroptosis [44]. FTH1, as a key ferroptosis factor, could restrain ferroptosis to drive gastric cancer progression [45]. However, the role of GCH1 or FTH1 in TNBC cell ferroptosis and its involvement in DOX resistance are completely unknown. In this work, FTH1 and GCH1 were screened out in ZFP64-depleted TNBC cells due to the most down-regulation efficiency. Furthermore, ZFP64 directly bound to FTH1 and GCH1 promoters and promoted their transcription. Further studies revealed that FTH1 and GCH1 participated in chemoresistance of tumor cells [46, 47]. Consistently, we found that FTH1 or GCH1 overexpression counteracted shZFP64-induced ferroptosis and DOX sensitivity in TNBC cells. Hence, these observations suggested that ZFP64 repressed ferroptosis via activating FTH1-mediated depletion of intracellular Fe^{2+} or GCH1-meidated lipid peroxidation inhibition, which was responsible for TNBC cell chemoresistance.

There are several limitations in this study. Beyond ferroptosis regulation, ZFP64 has broader effects on cancer progression through other mechanisms, such as glycolysis [48], immune evasion [23], and so on. Whether ZFP64 contributed to DOX resistance of TNBC cells via other mechanisms needs to be explored in the future. Besides, increasing proof has suggested that various inducers and pathways can modulate ferroptosis in cancer therapeutics [49]. Thus, other alternative pathways that can influence ferroptosis during DOX resistance of TNBC cells remain obscure.

Taken together, our findings demonstrated that CAFs-derived lactate facilitated ZFP64 histone lactylation to confer DOX resistance of TNBC, which was mediated through GCH1 and FTH1-mediated suppressive ferroptosis via regulation of iron metabolism and lipid peroxidation. This study deepened the understanding of the complicated mechanisms of CAFs-mediated chemoresistance of TNBC cells, further highlighting that targeting ZFP64 might be a promising therapeutic strategy for overcoming DOX resistance. Future research directions should focus on other potential mechanisms of ZFP64, as well as alternative pathways that may regulate ferroptosis during DOX resistance of TNBC cells. Besides, our

experimental findings highlighted the need for further research in humanized models to overcome translational challenges and optimize therapeutic efficacy.

Abbreviations

TNBC	Triple-negative breast cancer
DOX	Doxorubicin
GCH1	GTP cyclohydrolase-1
FTH1	Ferritin heavy chain 1
CAFs	Cancer-associated fibroblasts
ZFP64	Zinc finger protein 64
LA	Lactic acid
Fer-1	Ferrostain-1
DFO	Deferoxamine
Nec-1	Necrostain-1
shRNA	Short hairpin RNA
shNC	Negative control shRNA
CCK-8	Cell counting Kit-8
PI	Propidium iodide
GSH	Glutathione
MDA	Malondialdehyde
Fe^{2+}	Ferrous iron
TEM	Transmission electron microscope
ChIP	Chromatin Immunoprecipitation
DAB	Diaminobenzidine
RT-qPCR	Quantitative Real-Time PCR
SD	Standard deviation
ANOVA	Analysis of variance
ROS	Reactive oxygen species
PI	Propidium iodide
HMGB1	High-mobility group box-1
YTHDF2	YTH m6A RNA-binding protein 2
FBS	Fetal bovine serum
FAP	Fibroblast activated protein
α-SMA	Smooth muscle actin-alpha
ATCC	American Type Culture Collection
GAPDH	Glyceraldehyde-phosphate dehydrogenase

Supplementary Information

The online version contains supplementary material available at https://doi.org/10.1186/s12967-025-06246-3.

Supplementary Material 1

Supplementary Material 2

Supplementary Material 3

Supplementary Material 4

Supplementary Material 5

Supplementary Material 6

Author contributions

KeJing Zhang and Na Luo designed this study. KeJing Zhang, Lei Guo, Xin Li and Yu Hu collected the materials and performed the experiments. KeJing Zhang and Na Luo analysed the data and wrote the manuscript. Na Luo revised the manuscript. All authors read and approved the final version of the manuscript.

Funding

None.

Data availability

All data generated or analysed during this study are included in this published article.

Declarations

Ethics approval and consent to participate

Written informed consent was collected from all participants. This study was approved by the Xiangya Hospital, Central South University. The animal experiments were approved by the Experimental Ethics Committee Xiangya Hospital, Central South University.

Consent for publication

The informed consent obtained from study participants.

Conflict of interest

The authors declare that they have no conflict of interest.

Received: 28 September 2024 / Accepted: 11 February 2025
Published online: 28 February 2025

References

1. Hu Y, He Y, Luo N, Li X, Guo L, Zhang K. A feedback loop between lncRNA MALAT1 and DNMT1 promotes triple-negative breast cancer stemness and tumorigenesis. Cancer Biol Ther. 2023;24:2235768.
2. Dong H, Gao M, Lu L, Gui R, Fu Y. Doxorubicin-loaded platelet decoys for enhanced Chemoimmunotherapy Against Triple-negative breast Cancer in mice Model. Int J Nanomed. 2023;18:3577–93.
3. Diana A, Carlino F, Franzese E, Oikonomidou O, Criscitiello C, De Vita F, Ciardiello F, Orditura M. Early triple negative breast Cancer: Conventional Treatment and emerging therapeutic landscapes. Cancers (Basel) 2020, 12.
4. Chen Y, Feng X, Yuan Y, Jiang J, Zhang P, Zhang B. Identification of a novel mechanism for reversal of doxorubicin-induced chemotherapy resistance by TXNIP in triple-negative breast cancer via promoting reactive oxygen-mediated DNA damage. Cell Death Dis. 2022;13:338.
5. Niu J, Xue A, Chi Y, Xue J, Wang W, Zhao Z, Fan M, Yang CH, Shao ZM, Pfeffer LM, et al. Induction of miRNA-181a by genotoxic treatments promotes chemotherapeutic resistance and metastasis in breast cancer. Oncogene. 2016;35:1302–13.
6. Tang J, Long G, Li X, Zhou L, Zhou Y, Wu Z. The deubiquitinase EIF3H promotes hepatocellular carcinoma progression by stabilizing OGT and inhibiting ferroptosis. Cell Commun Signal. 2023;21:198.
7. Luo B, Zheng H, Liang G, Luo Y, Zhang Q, Li X. HMGB3 contributes to Anti-PD-1 resistance by inhibiting IFN-gamma-driven ferroptosis in TNBC. Mol Carcinog 2024.
8. Ye P, Wang C, Wen Y, Fang K, Li Q, Zhang X, Yang J, Li R, Chen M, Tong X, et al. A positive-feedback loop suppresses TNBC tumour growth by remodeling tumour immune microenvironment and inducing ferroptosis. Biomaterials. 2025;315:122960.
9. Zhu H, Jiang CW, Zhang WL, Yang ZY, Sun G. Targeting oncogenic MAGEA6 sensitizes triple negative breast cancer to doxorubicin through its autophagy and ferroptosis by stabling AMPKalpha1. Cell Death Discov. 2024;10:430.
10. Gong G, Ganesan K, Liu Y, Huang Y, Luo Y, Wang X, Zhang Z, Zheng Y. Danggui Buxue Tang improves therapeutic efficacy of doxorubicin in triple negative breast cancer via ferroptosis. J Ethnopharmacol. 2024;323:117655.
11. Peng L, Wang D, Han Y, Huang T, He X, Wang J, Ou C. Emerging role of Cancer-Associated fibroblasts-derived exosomes in Tumorigenesis. Front Immunol. 2021;12:795372.
12. Amornsupak K, Insawang T, Thuwajit P, Eccles POC, Thuwajit SA. Cancer-associated fibroblasts induce high mobility group box 1 and contribute to resistance to doxorubicin in breast cancer cells. BMC Cancer. 2014;14:955.
13. Lawal B, Wu AT, Chen CH, T AG, Wu SY. Identification of INFG/STAT1/NOTCH3 as gamma-mangostin's potential targets for overcoming doxorubicin resistance and reducing cancer-associated fibroblasts in triple-negative breast cancer. Biomed Pharmacother. 2023;163:114800.
14. Chen X, Song E. Turning foes to friends: targeting cancer-associated fibroblasts. Nat Rev Drug Discov. 2019;18:99–115.
15. Guo H, Ha C, Dong H, Yang Z, Ma Y, Ding Y. Cancer-associated fibroblast-derived exosomal microRNA-98-5p promotes cisplatin resistance in ovarian cancer by targeting CDKN1A. Cancer Cell Int. 2019;19:347.
16. Qi R, Bai Y, Li K, Liu N, Xu Y, Dal E, Wang Y, Lin R, Wang H, Liu Z, et al. Cancer-associated fibroblasts suppress ferroptosis and induce gemcitabine resistance in pancreatic cancer cells by secreting exosome-derived ACSL4-targeting miRNAs. Drug Resist Updat. 2023;68:100960.

17. He Y, Ji Z, Gong Y, Fan L, Xu P, Chen X, Miao J, Zhang K, Zhang W, Ma P, et al. Numb/Parkin-directed mitochondrial fitness governs cancer cell fate via metabolic regulation of histone lactylation. Cell Rep. 2023;42:112033.
18. Pan L, Feng F, Wu J, Fan S, Han J, Wang S, Yang L, Liu W, Wang C, Xu K. Demethylzeylasteral targets lactate by inhibiting histone lactylation to suppress the tumorigenicity of liver cancer stem cells. Pharmacol Res. 2022;181:106270.
19. Yu J, Chai P, Xie M, Ge S, Ruan J, Fan X, Jia R. Histone lactylation drives oncogenesis by facilitating m(6)a reader protein YTHDF2 expression in ocular melanoma. Genome Biol. 2021;22:85.
20. Sun K, Tang S, Hou Y, Xi L, Chen Y, Yin J, Peng M, Zhao M, Cui X, Liu M. Oxidized ATM-mediated glycolysis enhancement in breast cancer-associated fibroblasts contributes to tumor invasion through lactate as metabolic coupling. EBioMedicine. 2019;41:370–83.
21. He Z, Zhong Y, Hu H, Li F. ZFP64 promotes Gallbladder Cancer Progression through recruiting HDAC1 to Activate NOTCH1 Signaling Pathway. Cancers (Basel) 2023, 15.
22. Qiu G, Deng Y. ZFP64 transcriptionally activates PD-1 and CTLA-4 and plays an oncogenic role in esophageal cancer. Biochem Biophys Res Commun. 2022;622:72–8.
23. Wei CY, Zhu MX, Zhang PF, Huang XY, Wan JK, Yao XZ, Hu ZT, Chai XQ, Peng R, Yang X, et al. PKCalpha/ZFP64/CSF1 axis resets the tumor microenvironment and fuels anti-PD1 resistance in hepatocellular carcinoma. J Hepatol. 2022;77:163–76.
24. Zhu M, Zhang P, Yu S, Tang C, Wang Y, Shen Z, Chen W, Liu T, Cui Y. Targeting ZFP64/GAL-1 axis promotes therapeutic effect of nab-paclitaxel and reverses immunosuppressive microenvironment in gastric cancer. J Exp Clin Cancer Res. 2022;41:14.
25. Wang X, Chen T, Li C, Li W, Zhou X, Li Y, Luo D, Zhang N, Chen B, Wang L, et al. CircRNA-CREIT inhibits stress granule assembly and overcomes doxorubicin resistance in TNBC by destabilizing PKR. J Hematol Oncol. 2022;15:122.
26. Yang Y, Zhao Q, Peng Z, Zhou Y, Niu MM, Chen L. A GSH/CB dual-controlled self-assembled nanomedicine for high-efficacy doxorubicin-resistant breast Cancer Therapy. Front Pharmacol. 2021;12:811724.
27. Costa A, Kieffer Y, Scholer-Dahirel A, Pelon F, Bourachot B, Cardon M, Sirven P, Magagna I, Fuhrmann L, Bernard C, et al. Fibroblast heterogeneity and immunosuppressive environment in human breast Cancer. Cancer Cell. 2018;33:463–e479410.
28. Torres-Ruiz S, Tormo E, Garrido-Cano I, Lameirinhas A, Rojo F, Madoz-Gurpide J, Burgues O, Hernando C, Bermejo B, Martinez MT et al. High VEGFR3 expression reduces Doxorubicin Efficacy in Triple-negative breast Cancer. Int J Mol Sci 2023, 24.
29. Wang W, Li M, Ponnusamy S, Chi Y, Xue J, Fahmy B, Fan M, Miranda-Carboni GA, Narayanan R, Wu J, Wu ZH. ABL1-dependent OTULIN phosphorylation promotes genotoxic Wnt/beta-catenin activation to enhance drug resistance in breast cancers. Nat Commun. 2020;11:3965.
30. Liang Y, Wang Y, Zhang Y, Ye F, Luo D, Li Y, Jin Y, Han D, Wang Z, Chen B, et al. HSPB1 facilitates chemoresistance through inhibiting ferroptotic cancer cell death and regulating NF-kappaB signaling pathway in breast cancer. Cell Death Dis. 2023;14:434.
31. Wang Z, Li R, Hou N, Zhang J, Wang T, Fan P, Ji C, Zhang B, Liu L, Wang Y et al. PRMT5 reduces immunotherapy efficacy in triple-negative breast cancer by methylating KEAP1 and inhibiting ferroptosis. J Immunother Cancer 2023, 11.
32. Sun C, Liu P, Pei L, Zhao M, Huang Y. Propofol inhibits proliferation and augments the Anti-tumor Effect of Doxorubicin and Paclitaxel partly through promoting ferroptosis in Triple-negative breast Cancer cells. Front Oncol. 2022;12:837974.
33. Sahai E, Astsaturov I, Cukierman E, DeNardo DG, Egeblad M, Evans RM, Fearon D, Greten FR, Hingorani SR, Hunter T, et al. A framework for advancing our understanding of cancer-associated fibroblasts. Nat Rev Cancer. 2020;20:174–86.
34. Jin Z, Lu Y, Wu X, Pan T, Yu Z, Hou J, Wu A, Li J, Yang Z, Li C, et al. The cross-talk between tumor cells and activated fibroblasts mediated by lactate/BDNF/TrkB signaling promotes acquired resistance to anlotinib in human gastric cancer. Redox Biol. 2021;46:102076.
35. Zhang H, Deng T, Liu R, Ning T, Yang H, Liu D, Zhang Q, Lin D, Ge S, Bai M, et al. CAF secreted miR-522 suppresses ferroptosis and promotes acquired chemo-resistance in gastric cancer. Mol Cancer. 2020;19:43.
36. Zhang Y, Peng Q, Zheng J, Yang Y, Zhang X, Ma A, Qin Y, Qin Z, Zheng X. The function and mechanism of lactate and lactylation in tumor metabolism and microenvironment. Genes Dis. 2023;10:2029–37.
37. Pandkar MR, Sinha S, Samaiya A, Shukla S. Oncometabolite lactate enhances breast cancer progression by orchestrating histone lactylation-dependent c-Myc expression. Transl Oncol. 2023;37:101758.
38. Sun X, He L, Liu H, Thorne RF, Zeng T, Liu L, Zhang B, He M, Huang Y, Li M et al. The diapause-like colorectal cancer cells induced by SMC4 attenuation are characterized by low proliferation and chemotherapy insensitivity. Cell Metab 2023.
39. Li SY, An P, Cai HY, Bai X, Zhang YN, Yu B, Zuo FY, Chen G. Proteomic analysis of differentially expressed proteins involving in liver metastasis of human colorectal carcinoma. Hepatobiliary Pancreat Dis Int. 2010;9:149–53.
40. Sugai T, Habano W, Endoh M, Konishi Y, Akasaka R, Toyota M, Yamano H, Koeda K, Wakabayashi G, Suzuki K. Molecular analysis of gastric differentiated-type intramucosal and submucosal cancers. Int J Cancer. 2010;127:2500–9.
41. Torti FM, Torti SV. Regulation of ferritin genes and protein. Blood. 2002;99:3505–16.
42. Zhang Y, Kong Y, Ma Y, Ni S, Wikerholmen T, Xi K, Zhao F, Zhao Z, Wang J, Huang B, et al. Loss of COPZ1 induces NCOA4 mediated autophagy and ferroptosis in glioblastoma cell lines. Oncogene. 2021;40:1425–39.
43. Kraft VAN, Bezjian CT, Pfeiffer S, Ringelstetter L, Muller C, Zandkarimi F, Merl-Pham J, Bao X, Anastasov N, Kossl J, et al. GTP cyclohydrolase 1/Tetrahydrobiopterin counteract ferroptosis through lipid remodeling. ACS Cent Sci. 2020;6:41–53.
44. Hu Q, Wei W, Wu D, Huang F, Li M, Li W, Yin J, Peng Y, Lu Y, Zhao Q, Liu L. Blockade of GCH1/BH4 Axis activates Ferritinophagy to mitigate the resistance of Colorectal Cancer to Erastin-Induced ferroptosis. Front Cell Dev Biol. 2022;10:810327.
45. Su Y, Liu J, Zheng Z, Shi L, Huang W, Huang X, Ye C, Qi J, Wang W, Zhuang H. NSUN5-FTH1 Axis inhibits ferroptosis to promote the growth of gastric Cancer cells. Cell Biochem Biophys 2023.
46. Wang S, Xia Y, Huang P, Xu C, Qian Y, Fang T, Gao Q. Suppression of GCH1 sensitizes ovarian Cancer and breast Cancer to PARP inhibitor. J Oncol. 2023;2023:1453739.
47. Shi Z, Yuan H, Cao L, Lin Y. AKT1 participates in ferroptosis vulnerability by driving autophagic degradation of FTH1 in cisplatin-resistant ovarian cancer. Biochem Cell Biol 2023.
48. Sun J, Liu J, Hou Y, Bao J, Wang T, Liu L, Zhang Y, Zhong R, Sun Z, Ye Y. ZFP64 drives glycolysis-mediated stem cell-like properties and tumorigenesis in breast cancer. Biol Direct. 2024;19:83.
49. Vijayarangam V, Gopalakrishnan Deviparasakthi MK, Balasubramanian P, Palaniyandi T, Ravindran R, Suliman M, Saeed M, Natarajan S, Sivaji A, Baskar G. Ferroptosis as a hero against oral cancer. Pathol Res Pract. 2024;263:155637.

Publisher's note

Springer Nature remains neutral with regard to jurisdictional claims in published maps and institutional affiliations.